ChemComm

Dynamic Article Links

Cite this: *Chem. Commun.*, 2012, **48**, 6535–6537

www.rsc.org/chemcomm

COMMUNICATION

Chemiluminescence excited photoelectrochemistry using graphene–quantum dots nanocomposite for biosensing†

Wenwen Tu, Wenjing Wang, Jianping Lei,* Shengyuan Deng and Huangxian Ju*

Received 23rd April 2012, Accepted 10th May 2012
DOI: 10.1039/c2cc32866f

Chemiluminescence was used as the exciting light source to construct a universal photoelectrochemical platform based on a reduced graphene oxide–CdS nanocomposite, which greatly improves the photovoltaic transfer efficiency and leads to excellent performance for the photoelectrochemical immunoassay.

Photoelectrochemical measurement has attracted considerable attention as a newly developed and promising analytical technique.[1] Different from electrochemiluminescent (ECL)[2] and chemiluminescent (CL)[3] analyses, which detect the optical signal produced from analyte-intervenient electrochemical and chemical reactions, respectively, photoelectrochemical analysis uses a beam of excitation light to induce the detectable photoelectronic transfer between photoelectrochemically-active species and an electrode. The complete separation of excitation source (light) and detection signal (current) can greatly reduce the undesired background signal. Thus photoelectrochemical biosensing possesses highly sensitive detection performance, and a series of photoelectrochemical platforms have been designed for the detection of anti-cholera toxin antibody,[1b] nucleotides,[1c] H_2O_2,[1d] glutathione,[1e] thrombin,[1f] and cysteine.[1g] However, a physical light source makes the instrument and detection process complicated. Sometimes, a monochromator is also required to bring appropriate light emission to excite various photoelectrochemically active materials. These limits are unfavorable for the miniaturization of detection devices and *in situ* detection by photoelectrochemistry. Therefore, it is desirable to seek a substitute for a physical light source for exciting with a specific wavelength.

CL emission is a promising substitute for the physical light source. The oxidation of luminol with H_2O_2 is one of the most commonly known CL reactions. It has been used to excite quantum dots (QDs) to generate CL resonance energy transfer for the optical read-out of recognition events[3] and photocurrent for the determination of thiols in cancer cells.[4] Adjusting the reaction conditions of CL systems can bring light emission with different wavelengths to realize photoelectrochemical detection without the need of a physical light source and monochromator. Herein, a CL excited photoelectrochemical analytical protocol was designed by combining a gold nanoparticle (AuNP) enhanced CL system of luminol–H_2O_2–horseradish peroxidase (HRP)–*p*-iodophenol (PIP) as the luminescence donor (Scheme 1). This protocol introduced the photocurrent transfer system of QDs to immunological recognition, producing a novel biosensing strategy. The AuNPs could not only be used as a carrier of luminol and HRP but also catalyze the CL reaction,[5] which greatly enhanced the CL emission. This design greatly simplified the analytical apparatus and realized physical light source-free photoelectrochemical detection.

To improve the efficiency of photocurrent transfer, a nanocomposite of CdS QDs and reduced graphene oxide (RGO) was prepared by one-pot reaction as the photoelectrochemical probe (RGO–CdS), which was coated on a fluorine-doped tin oxide (FTO) electrode for the measurement of photocurrent. Using carcinoembryonic antigen (CEA) as a model, the anti-CEA antibody (Ab_1) was bound to the RGO–CdS coating. After a sandwich immunoreaction, the HRP labeled anti-CEA antibody (Ab_2) and luminol functionalized AuNPs were assembled on the FTO surface for performing the CL excited photoelectrochemical immunoassay. This strategy not only extends the applications of photoelectrochemistry, but also presents a novel methodology for bioassays.

The Fourier-transform infrared spectrum (FTIR) of graphene oxide (GO) showed four obvious peaks at 1110, 1380, 1630

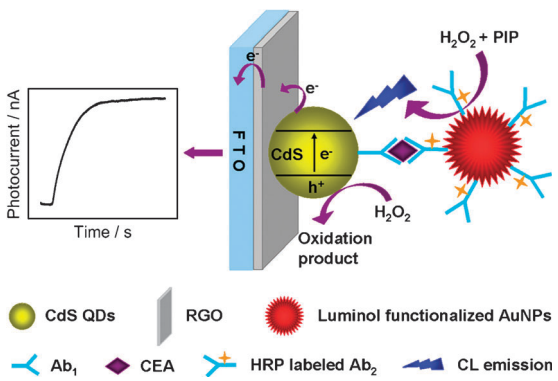

Scheme 1 Schematic illustration of the photoelectrochemical platform excited by chemiluminescence for biosensing.

State Key Laboratory of Analytical Chemistry for Life Science, School of Chemistry and Chemical Engineering, Nanjing University, Nanjing 210093, P.R. China. E-mail: hxju@nju.edu.cn; jpl@nju.edu.cn; Fax: +86-25-83593593; Tel: +86-25-83593593

† Electronic supplementary information (ESI) available: Experimental details, morphology characterization, CL spectrum, optimal conditions and clinical sample detection. See DOI: 10.1039/c2cc32866f

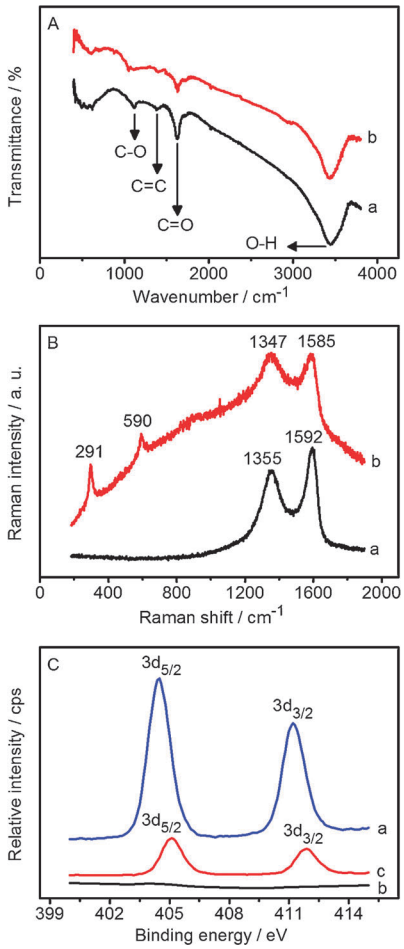

Fig. 1 (A) FTIR and (B) Raman spectra of (a) GO and (b) RGO–CdS nanocomposite; (C) Cd3d XPS of (a) CdS QDs, (b) GO, and (c) RGO–CdS nanocomposite.

and 3445 cm^{-1} representing the stretching vibrations of C–O, C=C, carboxyl or conjugated carbonyl groups on the edge of the layer plane, and hydroxyl groups of GO,[6] respectively (Fig. 1A, curve a). After the one-pot reaction of GO with H_2S in the presence of Cd^{2+}, the intensity of the carboxyl groups obviously decreased, while the other peaks were almost constant, indicating the reduction of GO sheets to RGO sheets during the *in situ* assembly of CdS QDs on the RGO sheets (Fig. 1A, curve b). The formation of RGO could improve photocurrent transfer efficiency and electron transfer between CdS QDs and the electrode surface for the measurement of photocurrent.[7]

Raman spectra demonstrated the formation of RGO–CdS nanocomposite. The Raman spectrum of GO showed a disorder-induced D-band at 1355 cm^{-1} arising from sp^3-hybridized carbon and a tangential stretch G-band at 1592 cm^{-1} representing the E_{2g} zone center mode of crystalline graphite (Fig. 1B, curve a), indicating significant edge-plane-like defective sites existing on the surface of GO.[8] After the one-pot reaction, the D and G bands shifted to 1347 and 1585 cm^{-1}, respectively, and two characteristic absorption peaks occurred at 291 and 590 cm^{-1} (Fig. 1B, curve b). Since the G-band position is known to be sensitive to electron or hole doping,[9] the observed red-shift of the G-band by 7 cm^{-1} implied good electron communication between the RGO sheet and CdS QDs. The new peaks could be assigned as the fundamental longitudinal optical phonon mode of CdS QDs and the breathing mode of the ligand itself, respectively.[10] These results suggested that CdS QDs were *in situ* assembled on RGO sheets.

The assembly of CdS QDs on RGO was further confirmed from X-ray photoelectron spectra (XPS) (Fig. 1C). The typical Cd3d XPS of CdS QDs showed a doublet structure due to the spin–orbit splitting, which was assigned to the $3d_{5/2}$ and $3d_{3/2}$ with a binding energy separation of 6.7 eV (curve a), while no obvious signal was observed in the XPS of GO (curve b). In comparison with the Cd3d XPS of CdS QDs, the binding energy for the $3d_{5/2}$ and $3d_{3/2}$ spin orbit of the RGO–CdS nanocomposite shifted to a higher energy from 404.5 eV and 411.2 eV to 405.1 and 411.9 eV, respectively (curve c), due to the electron transfer from CdS QDs to the RGO sheet.[9a] These results confirmed that CdS QDs deposited on the RGO sheet, which was consistent with the TEM image (Fig. S1 in ESI†). The highly dense deposits of CdS QDs on the graphene sheet were beneficial for photoelectron transfer between CdS QDs and RGO.

After the designed RGO–CdS nanocomposite was coated on the FTO electrode, the photoelectronic communication could be detected by a CL excitation, which was produced from the oxidation of luminol by H_2O_2 in the presence of HRP. As shown in Scheme 1, the luminol and HRP labeled Ab_2 functionalized AuNPs as the detection probe could be bound to the Ab_1 bound electrode surface by a sandwich immunoreaction. Upon addition of H_2O_2, the CL was produced and used as an exciting light source to induce the electron transfer from QDs to RGO and then to the FTO electrode. The photoelectrochemical responses were recorded for the immunoassay at an applied potential of +0.2 V, which is closer to physiological potential than −1.45 V for ECL immunosensing,[2a] leading to less interference. The relatively lower applied potential was attributed to the irradiation to produce electron–hole pairs, and the electrons transferred to the electrode to produce photocurrent which was different from ECL. The intensity of the photocurrent remarkably depended on the amount of HRP bound to the electrode surface, leading to a simple photoelectrochemical platform for the immunoassay of an analyte. After the Ab_1 bound electrode was incubated with 0.5 ng mL^{-1} CEA and then the detection probe, the photocurrent of 141.8 nA could be observed at 5 mM H_2O_2, which was about 22 times higher than 6.2 nA observed without target CEA (Fig. S2 in ESI†), indicating efficient association of the detection probe on the biosensor surface. The small photocurrent observed in the absence of CEA was due to the nonspecific adsorption of the detection probe.

The CL spectrum of the luminol–H_2O_2–HRP–PIP system showed a maximum emission wavelength at about 427 nm (Fig. S3 in ESI†), at which CdS QDs could be excited to produce photoinduced electron transfer.[1h] Here PIP was a CL intensifier. The stable CL emission could maintain for about 500 s; afterward the photocurrent decreased (Fig. S4 in ESI†). Under illumination of the CL emission, CdS QDs were irradiated to produce electron–hole pairs by exciting the electrons from the valence band to the conduction band.

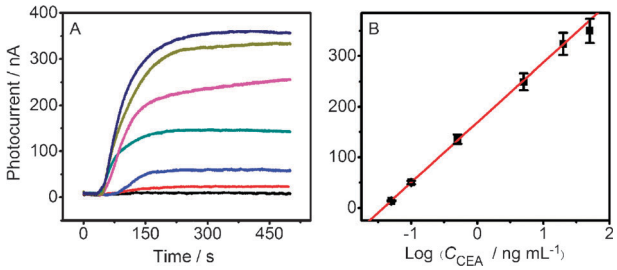

Fig. 2 (A) Photoelectrochemical responses of the immunosensor to 0, 0.05, 0.1, 0.5, 5, 20 and 50 ng mL^{-1} CEA at the applied potential of +0.2 V, and (B) linear calibration.

The conduction-band electrons were then injected into RGO and the FTO electrode, leading to the photocurrent. The formed valence-band holes of the CdS QDs could obtain electrons from H_2O_2 as an electron donor, which inhibited the photocorrosion of CdS QDs, completing the photocurrent generation cycle.

In the absence of RGO, the Ab_1 bound CdS QDs coating showed a photocurrent of 41.0 nA after incubation with target CEA and detection probe (Fig. S2 in ESI,† curve c). The photocurrent was much lower than that of the RGO–CdS coating, indicating the efficient improvement of the photocurrent transfer efficiency by RGO.[1f] Therefore, RGO could serve as a good photoelectron acceptor to improve the activity of CdS QDs due to its excellent capacity of photoinduced electron transport, and inhibition of the charge recombination of excited CdS.[1f]

Under the optimal conditions in tris-HCl buffered saline (pH 8.5) with an incubation time of 35 min (Fig. S5 in ESI†) and the applied potential of +0.2 V (Fig. S6 in ESI†), the typical time-based photocurrent response of the light source-free photoelectrochemical immunosensor to analyte was demonstrated at different concentrations of CEA (Fig. 2). A good linear relationship between the photocurrent and the logarithm value of CEA concentration ranging from 0.05 to 20 ng mL^{-1} was observed. The regression equation was $I = 166.8 + 117.8\log C$ with a correlation coefficient of 0.9995, where I is the photocurrent of the photoelectrochemical biosensor in the presence of CEA, and C is the concentration of CEA. The detection limit at a signal-to-noise ratio of 3 was calculated to be 0.01 ng mL^{-1}. The linear range was much wider than 1.0–60 ng mL^{-1} by the CL method.[11] The detection limit was lower than 0.39 ng mL^{-1} by the CL method,[11] 0.2 ng mL^{-1} by the electrochemical method,[12] and 0.5 ng mL^{-1} by the ECL method.[2b] Since the normal level of CEA in human serum is in the range of 3–5 ng mL^{-1},[12] this photoelectrochemical platform was more suitable for practical application.

The coefficients of variation for five times measurements of 0.1 and 5.0 ng mL^{-1} CEA using five CL excited photoelectrochemical immunosensors were 8.2% and 7.6% (electrode-to-electrode), respectively, indicating acceptable precision and fabrication reproducibility. When the biosensor was stored in shade at 4 °C for two weeks, 90.3% of its initial photocurrent response was maintained, suggesting acceptable stability and reproducibility. Results from real serum sample measurements validate the feasibility of the proposed strategy (Table S1 in ESI†).

In summary, using chemiluminescence as an exciting light source, a universal photoelectrochemical platform was successfully constructed. By combining with biological recognition, the platform could be conveniently developed for biosensing. Using luminol and HRP-Ab_2 functionalized AuNPs as a detection probe and an Ab_1 bound RGO–CdS modified FTO electrode as the immunosensor, the proposed immunoassay method showed excellent performance. The presence of graphene greatly improved the photocurrent transfer efficiency. Since different CL systems can produce different emission wavelengths, the designed strategy has an expansive and promising perspective of application in other photoelectrochemically-active materials for the construction of versatile photoelectrochemical platforms.

This research was financially supported by the National Basic Research Program of China (2010CB732400), the NNSF of China (21135002, 21075060, 21121091), the program for New Century Excellent Talents in University (NCET100479), and the Science Foundation of Jiangsu (BK2010302).

Notes and references

1 (*a*) R. Gill, M. Zayats and I. Willner, *Angew. Chem., Int. Ed.*, 2008, **47**, 7602; (*b*) N. Haddour, J. Chauvin, C. Gondran and S. Cosnier, *J. Am. Chem. Soc.*, 2006, **128**, 9693; (*c*) A. Ikeda, M. Nakasu, S. Ogasawara, H. Nakanishi, M. Nakamura and J. Kikuchi, *Org. Lett.*, 2009, **11**, 1163; (*d*) D. Chen, H. Zhang, X. Li and J. H. Li, *Anal. Chem.*, 2010, **82**, 2253; (*e*) W. W. Tu, Y. T. Dong, J. P. Lei and H. X. Ju, *Anal. Chem.*, 2010, **82**, 8711; (*f*) X. R. Zhang, S. G. Li, X. Jin and S. S. Zhang, *Chem. Commun.*, 2011, **47**, 4929; (*g*) Y. T. Long, C. Kong, D. W. Li, Y. Li, S. Chowdhury and H. Tian, *Small*, 2011, **7**, 1624; (*h*) G. L. Wang, J. J. Xu, H. Y. Chen and S. Z. Fu, *Biosens. Bioelectron.*, 2009, **25**, 791.

2 (*a*) L. L. Li, K. P. Liu, G. H. Yang, C. M. Wang, J. R. Zhang and J. J. Zhu, *Adv. Funct. Mater.*, 2011, **21**, 869; (*b*) L. Ge, J. X. Yan, X. R. Song, M. Yan, S. G. Ge and J. H. Yu, *Biomaterials*, 2012, **33**, 1024.

3 R. Freeman, X. Q. Liu and I. Willner, *J. Am. Chem. Soc.*, 2011, **133**, 11597.

4 C. F. Ding, H. Li, X. L. Li and S. S. Zhang, *Chem. Commun.*, 2010, **46**, 7990.

5 S. Bi, Y. M. Yan, X. Y. Yang and S. S. Zhang, *Chem.–Eur. J.*, 2009, **15**, 4704.

6 C. Nethravathi, T. Nisha, N. Ravishankar, C. Shivakumara and M. Rajamathi, *Carbon*, 2009, **47**, 2054.

7 Y. X. Xu, H. Bai, G. W. Lu, C. Li and G. Q. Shi, *J. Am. Chem. Soc.*, 2008, **130**, 5856.

8 D. C. Wei, Y. Q. Liu, H. L. Zhang, L. P. Huang, B. Wu, J. Y. Chen and G. Yu, *J. Am. Chem. Soc.*, 2009, **131**, 11147.

9 (*a*) Y. T. Kim, J. H. Han, B. H. Hong and Y. U. Kwon, *Adv. Mater.*, 2010, **22**, 515; (*b*) S. Pisana, M. Lazzeri, C. Casiraghi, K. S. Novoselov, A. K. Geim, A. C. Ferrari and F. Maur, *Nat. Mater.*, 2007, **6**, 198.

10 R. Shen, X. Q. Shen, Z. M. Zhang, Y. S. Li, S. Y. Liu and H. W. Liu, *J. Am. Chem. Soc.*, 2010, **132**, 8627.

11 Z. J. Yang, H. Liu, C. Zong, F. Yan and H. X. Ju, *Anal. Chem.*, 2009, **81**, 5484.

12 N. Laboria, A. Fragoso, W. Kemmner, D. Latta, O. Nilsson, M. L. Botero, K. Drese and C. K. O'Sullivan, *Anal. Chem.*, 2010, **82**, 1712.